Available online at www.sciencedirect.com
SCIENCE DIRECT
Journal of Crystal Growth 248 (2003) 194–200
JOURNAL OF CRYSTAL GROWTH
www.elsevier.com/locate/jcrysgro

In-situ determination of interface roughness in MOVPE-grown visible VCSELs by reflectance spectroscopy

K. Haberland[a,b,*], M. Zorn[c], A. Klein[c], A. Bhattacharya[c,1], M. Weyers[c], J.-T. Zettler[b], W. Richter[a]

[a] *Technische Universität Berlin, Institut für Festkörperphysik, Sekr. PN 6-1, Hardenbergstr. 36, D-10623 Berlin, Germany*
[b] *LayTec GmbH für in-situ und Nano-Sensorik, Helmholtzstr. 13-14, D-10587 Berlin, Germany*
[c] *Ferdinand-Braun-Institut für Höchstfrequenztechnik, Albert-Einstein-Str. 11, D-12489 Berlin, Germany*

Abstract

This paper reports on an in-situ optical reflectance study of the development of the interface roughness of AlGaAs/AlAs distributed Bragg reflectors during the metalorganic vapour phase epitaxy growth of visible vertical-cavity surface-emitting laser structures. We show that the surface roughness can be extracted from time-resolved UV reflectance measurements. The roughness of the surface during growth for both the AlGaAs and AlAs layers can be determined individually. The values estimated from the in-situ optical data correlate well with the roughness measured ex-situ using atomic force microscopy. The in-situ reflectance measurement is thus shown to be a convenient non-invasive and non-destructive technique for determining surface and interface roughness even for complex device structures.
© 2002 Elsevier Science B.V. All rights reserved.

PACS: 81.05.Ea; 81.15.Gh; 42.55.Px; 78.66.Fd; 78.40.Fy; 78.20.Bh; 81.70.Fy

Keywords: A1. In-situ monitoring; A1. Surface and interface roughness A3. Metalorganic vapor phase epitaxy; B3. Vertical cavity surface emitting lasers

1. Introduction

Vertical-cavity surface-emitting lasers (VCSELs) have intrinsic properties that enable simpler fabrication, lower cost, and easier system integration than traditional edge-emitting lasers [1]. Consequently, VCSELs are the desired laser sources for a variety of optoelectronic technologies. 850 nm-emitting devices are already the preferred choice for gigabit-ethernet optical links and 650 nm visible-wavelength VCSELs are ideally suited for plastic fiber-based communication.

The VCSEL geometry with a short active region requires high reflectivities (>99.5%) of the mirrors sandwiching the cavity to achieve a reasonable threshold current density. Such a high reflectance is usually provided by quarter-wave $Al_xGa_{1-x}As/AlAs$ distributed Bragg reflector

*Corresponding author. LayTec GmbH für in-situ und Nano-Sensorik, Helmholtzstr. 13-14, D-10587 Berlin, Germany. Fax: +49-30-31808237.
E-mail address: haberland@laytec.de (K. Haberland).

[1] Solid State Electronics Group, Tata Institute of Fundamental Research, Homi Bhabha Road, Mumbai 400 005, India.

0022-0248/03/$ - see front matter © 2002 Elsevier Science B.V. All rights reserved.
PII: S0022-0248(02)01816-X

(DBR) mirrors. At $\lambda \sim 650\,\text{nm}$, an Al concentration $x \geqslant 0.5$ is necessary in the high-index layer for sufficient transparency, thus reducing the refractive index contrast and requiring a large number of DBR periods to achieve high reflectivity. Visible VCSELs often employ 50–55 pairs in the lower n-DBR and $\sim$35 pairs in the upper p-DBR thus making the total structure extremely thick ($\sim$8–9 mm) [2]. Fig. 1a shows a schematic cross section of the VCSEL structure. Furthermore, for low electrical resistance the DBR mirrors often employ alloy grading at interfaces, especially on the p-side [3]. Thus the VCSEL structure raises particularly difficult growth issues, and for such a stack with > 150 layers, control over the roughness each of the interfaces is crucial in determining the final reflectivity of the mirrors and eventually the device performance.

In-situ reflectometry is routinely used to monitor the growth of VCSEL structures, with the primary aim of assessing growth rates and the positions of the reflectivity maximum and the cavity resonance [4,5]. In this paper, we show that a careful analysis of the reflectivity data can also be used to accurately estimate the surface roughness during growth. The values predicted in-situ from optical measurements are in good agreement with interface roughness values measured ex-situ using atomic force microscopy (AFM).

2. Experimental details

The VCSEL structures discussed in this work were grown in an Aixtron AIX 200/4 low-pressure metalorganic vapour phase epitaxy (MOVPE) system equipped with a LayTec EpiRAS 200 in-situ sensor capable of combined reflectance and reflectance anisotropy spectroscopy (RAS) measurements on rotating samples [6,7]. The VCSEL structures were grown at a temperature of $T = 770°\text{C}$ on epi-ready n^+ (1 0 0) GaAs substrates tilted 6° towards [1 1 1]A. As shown in Ref. [8] using substrates with an offcut angle of 6° resulted in smoother layers than using exactly oriented wafers. Further details of the growth parameters are also given in Ref. [8]. The $Al_{0.5}Ga_{0.5}As/AlAs$ DBR mirrors were grown without any growth interruptions or purging sequences at the interfaces as this was found to result in the best structural quality of the DBRs.

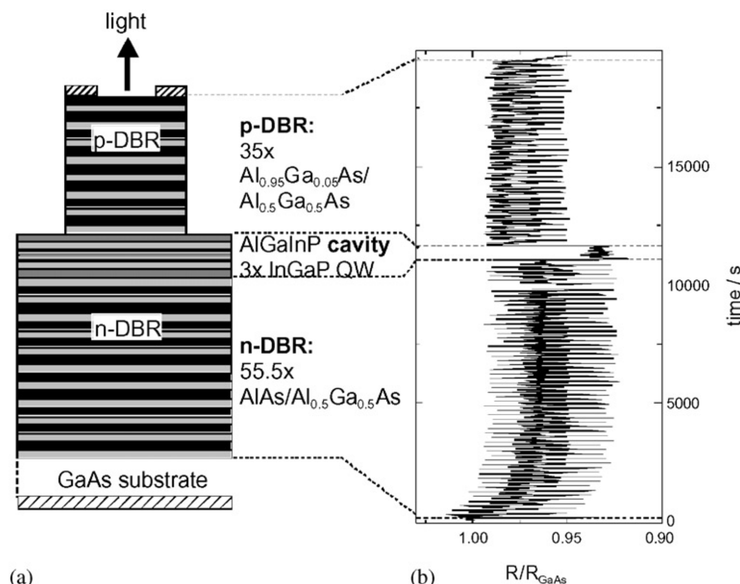

Fig. 1. (a) Schematic cross section of complete VCSEL structure and (b) corresponding normalized reflectance transient at $E = 4.0\,\text{eV}$ (310 nm) measured during growth at $T_{\text{nom}} = 770°\text{C}$.

2.1. Reflectance measurements

The entire growth of VCSEL structures has been monitored using the EpiRAS in-situ sensor by continuously taking both spectroscopic and time-resolved RAS and reflectance (R) data. The result is a comprehensive fingerprint of the growth process in total and has been already described in Ref. [5]. For the measurements presented here, however, a very high time resolution was required. Therefore, the growth was monitored in the time-resolved measurement mode at a single wave length (transient measurement).

In this paper, we utilize the normalized reflectance R/R_{ref}, which is the reflectance of the growing layer stack divided by the reflectance of a well-known reference sample inside the reactor (see ref. [9] for details). In this work, the GaAs substrate reflectance $R_{ref} = R_{GaAs}$ was measured prior to each growth process and used thereafter as reference:

$$R/R_{ref} = \frac{R_{stack}}{R_{GaAs}}. \quad (1)$$

The normalized reflectance can be simulated by a multi-layer model using a set of high-temperature dielectric functions.

Beyond the optical wobble compensation capabilities of the EpiRAS system [6], the remaining effect of the wobble on the reflectance signal has been further reduced by averaging the time-resolved reflectance signal over exactly one wafer revolution. The rotation period of the wafer was determined from the simultaneously measured RAS signal. The noise of the measured normalized reflectance signal was $\pm 3 \times 10^{-3}$.

To maximize the sensitivity of the reflectance data to the surface roughness and the compositional grading, a rather short wavelength of $\lambda = 310\,\text{nm}$ ($E = 4.0\,\text{eV}$) was chosen for the optical measurement. The light penetration depth into AlGaAs at this wavelength is only around 10 nm, which makes the optical measurement particularly sensitive to the uppermost layer and also eases the interpretation of the data.

In order to simulate the reflectance transients, the high-temperature dielectric function data ε_1, ε_2 for all materials involved at $E = 4.0\,\text{eV}$ (310 nm) had to be determined by a preceding set of epitaxial growth runs. For this purpose, three parameter fits (ε_1, ε_2, growth rate r) to Fabry–Perot oscillations measured during growth of different $Al_xGa_{1-x}As$ compositions were performed.

The simulations are based on a multi-layer model with plane-parallel interfaces from which the complex reflectance can be calculated numerically [10,11]. If needed, a surface or interface roughness has been simulated by introducing additional layers consisting of an effective medium approximation according to Bruggemann [12,13]. The thickness of these layers was a free parameter and has been used to control the magnitude of the roughness. Fits were performed using a least-square minimization procedure. All fits and simulations in this work were done with the commercially available AnalysR software.[2]

2.2. AFM measurements

To measure the roughness of the interfaces *within* the VCSEL structures after growth using AFM, the layer stack was first mechanically bevelled at an angle of $\sim 0.3°$, using a diamond lapping film with 0.1 μm grain size. This spreads out the ~ 50 nm thick DBR layers to about 10 μm at the bevelled edge.

To remove the polishing damage, and also expose the AlGaAs layers the samples were etched in 7.5% hydrofluoric acid (HF). As the etch rate in HF for AlAs is an order of magnitude higher than for AlGaAs, primarily the individual AlGaAs layers are exposed at the bevelled edge as ~ 10 μm wide terraces. This enables AFM observations to be carried out at various depths in the structure and thus permits a study of the development of the interface roughness during the growth of the VCSEL. Surface roughness of the layers was estimated from AFM images obtained using a Digital Instruments Nanoscope II AFM operating in tapping mode. The RMS value for roughness evaluated over a $10\,\mu m \times 10\,\mu m$ field was used in all cases.

[2] AnalysR, simulation and analysis software for spectroscopic thin films, LayTec GmbH, http://www.laytec.de.

3. Results and discussion

In Fig. 1 the complete reflectance transient measured during VCSEL growth is shown alongside a schematic cross section. During growth of the n-DBR, two phases can be seen: an initial development phase ($t < 3000$ s) where the reflectance signal decreases gradually and a second phase where the signal level is constant ($t = 3000-11000$ s). During growth of the p-DBR, the reflectance signal exhibits only one phase, although at a higher signal level compared to the n-DBR.

Fig. 2 gives details from the measured 4.0 eV (310 nm) reflectance transient shown in Fig. 1b. For both the n-DBR and the p-DBR the open dots represent the measured data, while the lines are simulations. The dashed line is a simulation without assuming any surface roughness. Although the layers in the n- and the p-DBR are differently doped, the reflectance transients can be directly compared, as the doping does not change

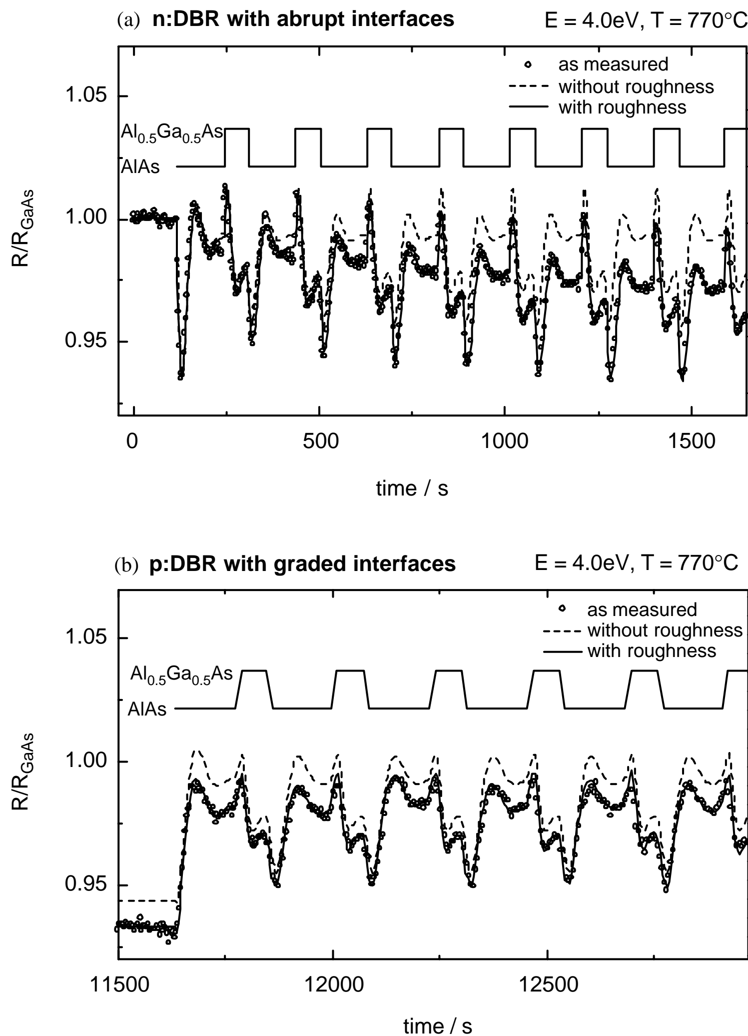

Fig. 2. Details of time-resolved normalized reflectance measurements of n-DBR (a) and p-DBR (b) together with a schematic composition profile. The dots represent the measured data, the lines show the simulations (dashed curve without surface roughness, solid curve including surface roughness).

the reflectance at this photon energy [14]. A comparison of the line shapes in Fig. 2a and b shows the most obvious differences to be the much sharper peaks and steeper slopes in the n-DBR. As discussed in Ref. [5] this is due to the abrupt interfaces between the n-DBR layers. In contrast, the interfaces between AlAs and $Al_{0.5}Ga_{0.5}As$ in the p-DBR (Fig. 2b) have been graded over a 10 nm region to reduce the series resistance [3,8]. They exhibit smoother transitions of the Fabry–Perot interferences. The grading was simulated with a step function using four layers of intermediate compositions, each 2 nm thick.

Due to the small penetration depth of the light at 4.0 eV (310 nm), exact periodicity of the reflectance transient for each pair of layers is expected, as was shown, e.g. in Ref. [15]. The simulation without roughness indeed shows this behaviour (Fig. 2a). Although agreeing well with the measured transient for the first pair of n-DBR layers, it shows increasing differences for the subsequent pairs of layers: the signal level of the whole transient decreases from layer pair to layer pair (see also Fig. 1b). In order to get agreement with the measured data, a surface roughness had to be assumed on top of the growing layer. When the layer was overgrown, the surface roughness transforms into an interface roughness and a surface roughness of the new layer. The surface roughness was simulated by using an effective medium formula according to Bruggeman [13] with a mixture of 50% voids in the host material. The thickness of the surface roughness layer was a free parameter and was fitted to the measurement, thus obtaining the roughness for each layer of the DBRs. The interface roughness was simulated by a Bruggemann effective medium mixture of the two adjacent layers. It turned out that the main effect on the reflectance transient arises from the surface roughness rather than from the overgrown interface roughness. That is not surprising, since both the penetration depth of the light and the difference in refractive index of the two materials is rather small at this photon energy. Therefore, the buried interface is only visible for thin overlayers.

For the n-DBR in Fig. 2a, an increasing roughness was found, that saturates at 3.5 nm after around 20 pairs. For the p-DBR, however, an almost constant roughness of approximately 2 nm was best fitting to the measured reflectivity data. The resulting effective medium roughness values obtained from the simulation, plotted against the number of DBR periods, are shown in Fig. 3. The increase in roughness during the growth of the n-DBR can be best fitted by a logarithmic function (solid and dashed curves in Fig. 3). Since the roughness fit can be performed for every single layer, one can even study differences in the roughness of the AlAs and the $Al_{0.5}Ga_{0.5}As$ layers. It turns out that the AlAs layers are slightly rougher than the $Al_{0.5}Ga_{0.5}As$ layers. This agrees with the expectation that a higher Ga content in the layer leads to smoother surfaces [16].

The cavity, consisting of 200 nm lattice-matched AlInGaP considerably smoothes the surface, as can be seen in Fig. 3 by the sudden drop in roughness after 55 pairs. The roughness of the following p-DBR is smaller than that of the n-DBR and also does not increase significantly during the growth of the stack. This behaviour could be attributed to indium that was introduced into the reactor during growth of the AlInGaP cavity. Further experiments where the cavity was grown before the n-DBR verified this assumption.

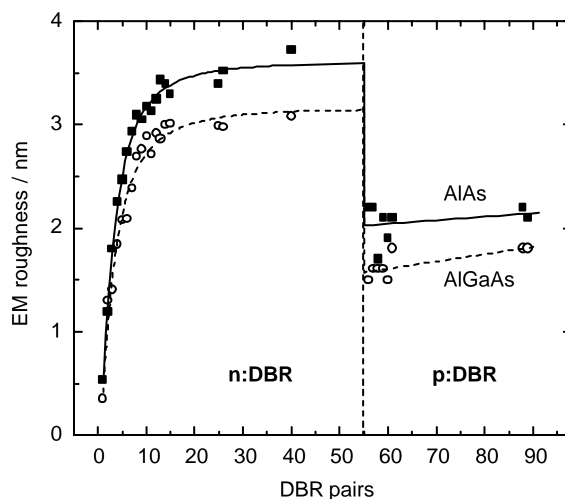

Fig. 3. Effective-medium roughness of the AlAs (solid squares) and AlGaAs (open circles) DBR layers determined from the reflectivity transient by fitting the measured data. The fit yields the roughness value with an accuracy of 0.1 nm.

The reflectance signal of the n-DBR grown after the cavity shows no decrease in reflectance and therefore no significant increase in roughness. This might be explained by the fact that indium is known to have a high diffusion length and to cause memory effects even in subsequent layers. Thus one possible explanation is that the p-DBR is smoothed due to the influence of the indium still present in the reactor and on the susceptor by some kind of "surfactant effect".

Fig. 4 shows the RMS roughness of the interfaces within two VCSEL structures as a function of depth (DBR periods) measured using the AFM technique discussed in the previous section. One is the VCSEL the optical measurements have been performed on, the other one is a nominally identical structure with a smaller number of DBR mirror pairs. The measured roughness belongs to the AlGaAs surfaces exposed at the bevelled edge. An independent measure of the roughness of the AlAs surface was not possible with the sample preparation method employed, due to limitations of the etchant. The trend seen in the development of the roughness from the reflectivity data is nicely verified by the AFM measurements: a rapid increase in roughness of the n-DBR in the first ~ 10 periods to a value of about 1.5 nm, followed by the remarkable drop in roughness after the growth of the AlGaInP-based cavity, and the relatively smaller roughness of the p-DBR. When comparing the *RMS roughness* from the AFM measurements with the *effective medium roughness* of the AlGaAs layers from the reflectance fit, it is important to keep in mind that the RMS roughness is a mean value, while the effective medium roughness is a peak-to-peak value. Therefore, the effective medium roughness should be higher than the RMS roughness by a factor of two, which is in agreement with our data (Figs. 3 and 4).

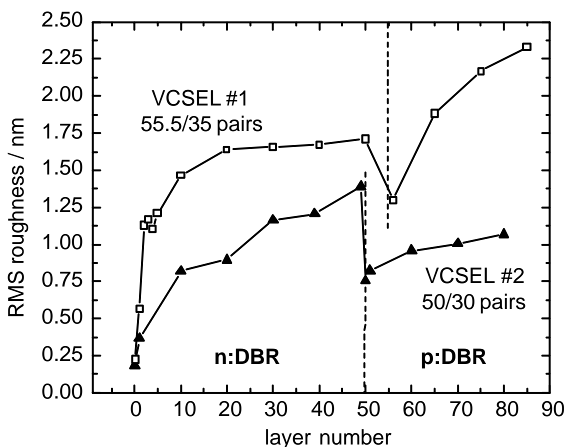

Fig. 4. RMS roughness depth profile determined by AFM measurements for two VCSEL structures. VCSEL #1 (open squares) is the one on which the optical measurements have been performed. VCSEL #2 (solid triangles) is shown to illustrate the relative accuracy of the AFM measurements. Apart from the different number of DBR pairs, both VCSELs nominally have the same structure.

The differences in RMS roughness between the two samples in Fig. 4 illustrate the systematic errors of the AFM measurement. Within the same sample, the error of the RMS value is rather small (approximately 0.1 nm). But comparability between the different samples is only possible with an uncertainty of about 1 nm. This uncertainty is based on the problems of the mechanical and wet chemical preparation of the sample. In this way, the differences between the two measured samples can be explained. The accuracy of the RMS roughness measurement may be somewhat smaller for the graded p-DBR. Since the grading on a microscopic scale can be regarded as statistical fluctuations of the Al-content, the selective etchant might produce an artificial roughness due to its selectivity and this will result in higher RMS values. This might explain why the roughness values determined by AFM are higher for the p-DBR than for the n-DBR. Since the in situ optical measurement does not show any indication for an increasing roughness in the p-DBR, we attribute this finding in the AFM roughness profile to the specific problems of the AFM measurement on high Al containing layers that were mentioned above.

In spite of the measured roughness, the devices fabricated from the structures discussed in this work demonstrate state-of-the-art performance for visible VCSELs [17], thus showing that the DBR mirrors achieve the necessary high reflectance even with the measured roughness values.

4. Conclusion

Valuable information about the surface and interface roughness of the DBR layers is contained in the measured reflectance data taken during growth and can be extracted from a simulation procedure. It is seen that the interface roughness quickly builds up and then saturates during the n-DBR growth. The AlGaInP cavity smoothens the surface remarkably, and the roughness does not increase considerably during the growth of the subsequent p-DBR mirror. The roughness estimated from the reflectivity measurements is in good agreement with the roughness measured ex situ using AFM. Such an in situ reflectance measurement is of course a non-invasive and non-destructive technique, offering additional advantages over the conventional AFM or TEM measurements. The observed interface roughness does not seem to have much impact on the device performance of the VCSEL.

Acknowledgements

The authors like to thank O. Fink for technical assistance at the MOVPE system. One of the authors (AB) is grateful for a research fellowship from the Alexander von Humboldt foundation.

References

[1] W.W. Chow, K.D. Choquette, M.H. Crawford, K.L. Lear, G.R. Hadley, IEEE J. Quantum Electron. QE-33 (1997) 1810.
[2] A. Knigge, M. Zorn, H. Wenzel, M. Weyers, Electron. Lett. 37 (2001) 1222.
[3] K.L. Lear, R.P. Schneider Jr., Appl. Phys. Lett. 62 (1996) 605.
[4] W.G. Breiland, H.Q. Hou, H.C. Chui, B.E. Hammons, J. Crystal Growth 174 (1997) 564.
[5] M. Zorn, K. Haberland, A. Knigge, A. Bhattacharya, M. Weyers, J.-T. Zettler, W. Richter, J. Crystal Growth 235 (2002) 25.
[6] K. Haberland, O. Hunderi, M. Pristovsek, J.-T. Zettler, W. Richter, Thin Solid Films 313–314 (1998) 620–624.
[7] K. Haberland, P. Kurpas, M. Pristovsek, J.-T. Zettler, M. Weyers, W. Richter, Appl. Phys. A 68 (1999) 309–313.
[8] A. Bhattacharya, M. Zorn, A. Oster, M. Nasarek, H. Wenzel, J. Sebastian, M. Weyers, G. Tränkle, J. Crystal Growth 221 (2000) 663.
[9] K. Haberland, A. Kaluza, M. Zorn, M. Pristovsek, H. Hardtdegen, M. Weyers, J.-T. Zettler, W. Richter, J. Crystal Growth 240 (2002) 87.
[10] F. Abelès, Ann. de Physique 5 (1950) 596 and 706.
[11] M. Born,E. Wolf, Principles of Optics, Pergamon Press, Oxford, 1987.
[12] D.A.G. Bruggemann, Ann. Phys. 24 (1935) 637.
[13] D.E. Aspnes, Phys. Rev. B 41 (1990) 10334.
[14] M. Kuball, M.K. Kelly, M. Cardona, K. Köhler, J. Wagner, Phys. Rev. B 49 (1994) 16569.
[15] G.N. Maracas, J.L. Edwards, D.S. Gerber, R. Droopad, Appl. Surf. Sci. 63 (1993) 1.
[16] S.F. Yoon, J. Electron. Electron. Eng. 13 (1993) 10.
[17] A. Knigge, M. Zorn, M. Weyers, G. Tränkle, Electron. Lett. 38 (2002) 882.